Journal of Alloys and Compounds xxx (2009) xxx–xxx

Contents lists available at ScienceDirect

Journal of Alloys and Compounds

journal homepage: www.elsevier.com/locate/jallcom

Thermal properties of Mg–11Y–5Gd–2Zn–0.5Zr (wt.%) alloy

C.J. Chen[a,1], Q.D. Wang[a,b,*], D.D. Yin[a]

[a] National Engineering Research Center of Light Alloy Net Forming, Shanghai Jiao Tong University, 800 Dongchuan Road, Shanghai 200240, PR China
[b] The State Key Laboratory of Metal Matrix Composites, Shanghai Jiao Tong University, 800 Dongchuan Road, Shanghai 200240, PR China

ARTICLE INFO

Article history:
Received 6 June 2009
Received in revised form 29 July 2009
Accepted 31 July 2009
Available online xxx

Keywords:
Mg–Y–Gd–Zn–Zr alloy
Specific heat capacity
Linear thermal expansion coefficient
Thermal conductivity
Thermal diffusivity

ABSTRACT

The specific heat capacity and linear thermal expansion coefficient of Mg–11Y–5Gd–2Zn–0.5Zr (wt.%) alloy after heat treatment were investigated in the range of 100–400 °C and 25–400 °C, respectively. Thermal conductivity and thermal diffusivity of the alloy were also measured at 25 °C, 200 °C and 300 °C. The results clearly show that the specific heat capacity and linear thermal expansion coefficient of the alloy increase with temperature, except for a peak value between 225 °C and 318 °C, which is caused by phase transformation. The values of the thermal conductivity and the thermal diffusivity of Mg–11Y–5Gd–2Zn–0.5Zr alloy at room temperature are 23.0 $W m^{-1} K^{-1}$ and $14.3 \times 10^{-6} m^2 s^{-1}$, respectively. The transitional element Y has an effective influence on the thermal conductivity and thermal diffusivity.

1. Introduction

Magnesium alloys are attractive as structural materials owing to their low density and high specific stiffness and strength at room temperature. However, the strength at elevated temperatures is limited. Adding some rare earth metals such as Y and Gd into Mg-base alloys can improve their strength and creep resistance at both room and elevated temperatures [1–4]. Gao et al. [5–7] have developed some kinds of high temperature resistant magnesium alloys, such as Mg–Y–Gd–Zr–(Zn), Mg–Gd–Y–Zr–(Zn). It was reported that the ultimate tensile strength of Mg–10Gd–2Y–0.5Zr (wt.%) alloy at room temperature was 402 MPa with extruded at 400 °C and the ultimate tensile strength of Mg–10Gd–3Y–1.0Zn–0.5Zr (wt.%) alloy at 250 °C was more than 320 MPa with extruded-T5 condition. [2,7]. These kinds of magnesium alloys would have great application on aerospace and automotive power system such as piston, which requires low density and high strength materials at high temperature [8,9]. The specific heat capacity, linear thermal expansion coefficient, thermal conductivity and thermal diffusivity are important thermophysical properties for magnesium alloy. They play an important role in the performance of magnesium alloys in structures and certain applications. There is a lack of studies for thermal properties of this high temperature resistant magnesium alloy. In the present study, the basic thermophysical properties of Mg–11Y–5Gd–2Zn–0.5Zr (wt.%) (WGZ115) alloy were investigated.

2. Experimental procedures

The Mg–11Y–5Gd–2Zn–0.5Zr (wt.%) (named as WGZ115) alloy was prepared by melting in an electrical resistance furnace protected by a mixed gas of CO_2 and SF_6 with the ratio of 100:1, and cast in steel moulds. The alloy was cast into steel moulds. All thermal properties of WGZ115 alloy were measured with different samples cut for the same ingot. All specimens were solution treated at 535 °C for 20 h, quenched into water with 25 °C, and then aged at 225 °C for 24 h in oil-bath. The actual chemical composition of the alloy was determined by an inductively coupled plasma analyzer (PerkinElmer, Plasma 400), and the results are listed in Table 1. Microstructures of the specimen were analyzed by JEM-6460 scanning electron microscopy (SEM) equipped with an energy dispersive X-ray spectrometer (EDX).

The DSC curve and specific heat capacity curve of WGZ115 alloy with the temperature range of 100–400 °C were carried out with a DSC 404C Pegasus (Differential Scanning Calorimeter). The specimen is a round plate with a size of $\Phi 4 \times 1.6$ mm and the heating rate is 10 °C/min. The linear thermal expansion coefficient of WGZ115 alloy was measured in argon atmosphere using the NETZSCH 402PC dilatometer from 25 °C to 400 °C. The specimen size is $\Phi 6 \times 25$ mm and the heating rate is 3 °C/min. The thermal diffusivity of the alloy was measured at 25 °C, 200 °C and 300 °C with a NETZSCH model LFA447 Flash Analyzer. The size of specimen is $\Phi 10 \times 2$ mm.

3. Results and discussion

3.1. Microstructures of WGZ115 alloy

The SEM image of WGZ115 alloy after solution treatment and aging treatment is shown in Fig. 1. It is observed that A is the α-Mg matrix, B is the residual $Mg_{24}(YGdZn)_5$ eutectic phase after solution

* Corresponding author at: National Engineering Research Center of Light Alloy Net Forming, Shanghai Jiao Tong University, 800 Dongchuan Road, Shanghai 200240, PR China. Tel.: +86 21 54742715; fax: +86 21 34202794.
E-mail addresses: chenyangtse@hotmail.com (C.J. Chen), wangqudong@sjtu.edu.cn, chenyangtse@gmail.com (Q.D. Wang).
[1] Tel.: +86 21 54742714.

0925-8388/$ – see front matter © 2009 Elsevier B.V. All rights reserved.
doi:10.1016/j.jallcom.2009.07.177

Table 1
Actual chemical composition of WGZ115 alloy.

Alloy	Composition/wt.% (at.%)				
	Y	Gd	Zn	Zr	Mg
WGZ115	11.3 (3.58)	4.66 (0.83)	2.01 (0.87)	0.34 (0.10)	Bal.

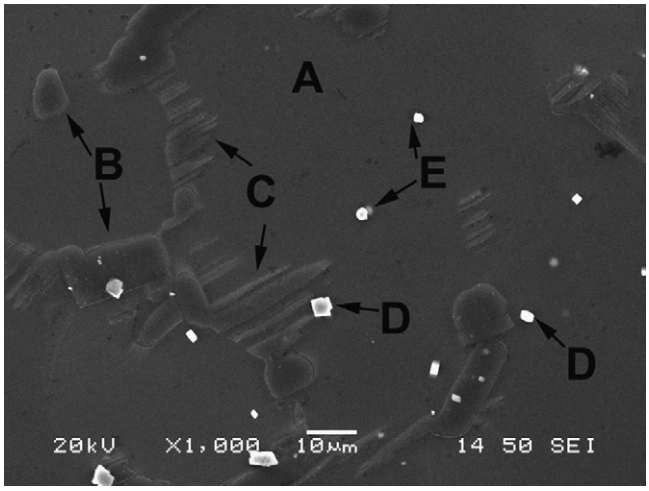

Fig. 1. SEM image of WGZ115 alloy after aging treatment.

treatment at 535 °C for 20 h and aging treatment at 225 °C for 24 h. C is the long-period stacking ordered structure phase $Mg_{12}Y_1Zn_1$ which uniformly distributes from the grain boundary to the inner of α-Mg. D is a cuboid-shaped phase which contains Y and Gd elements. It is distributed randomly near grain boundaries or in grain interior. E is the Zr-rich core and exists in grain interior [5].

3.2. Specific heat capacity

Fig. 2 shows the DSC curves of WGZ115 alloy and the reference measurements of the sapphire standard with the range of 100–400 °C. An endothermic peak appears between 225 °C and 318 °C in the chart. There are lots of small precipitated phases existing in grains after aged at 225 °C for 24 h. Those precipitates can only be relatively stable below 225 °C and change into another structure when temperature exceeds 225 °C.

Fig. 3 shows the specific heat capacity curve of WGZ115 alloy and theoretical calculation results are also given for comparison. It can be seen that the experimental results of specific heat capacity increase with increasing temperature except for a peak between 225 °C and 318 °C. At 100 °C, the value of testing results is 850 J/(kg K). It slowly rises to 982 J/(kg K) at 225 °C. It is perceptible that a peak appears because of phase transformation [10]. The values of specific heat capacity of the WGZ115 alloy rapidly increase when the temperature is higher than 318 °C.

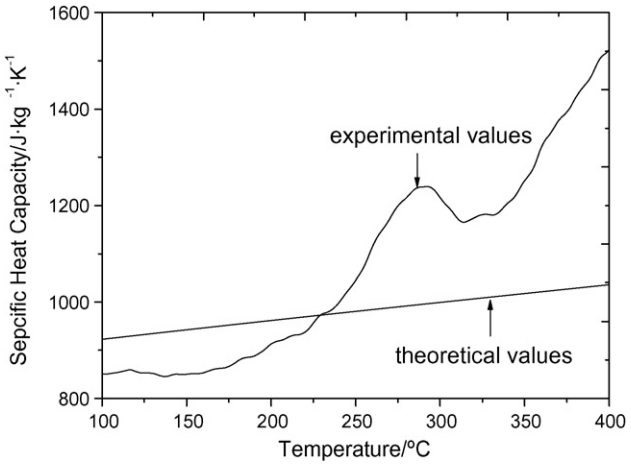

Fig. 3. Comparison of the measured and calculated curves of specific heat capacity.

The theoretical results of the specific heat capacity are calculated using Kopp–Neumann law which other authors have already demonstrated [11]. The equation is

$$C_p(T) = \sum C_{p,i}(T)x_i \quad (1)$$

where $C_{p,i}$ is the value for the specific heat capacity of the pure component and x_i is the mass ratio. The comparison shows that the measured and calculated value reached good agreement only at temperature below 225 °C. The small deviations are appropriately below 8.5%. The deviation is bigger when the temperature is above 225 °C. The calculated values of the specific heat capacity can be used below the phase transformation temperature.

3.3. Linear thermal expansion coefficient

Fig. 4 shows the relative elongation of WGZ115 alloy from 25 °C to 400 °C. The average linear thermal expansion coefficient is cal-

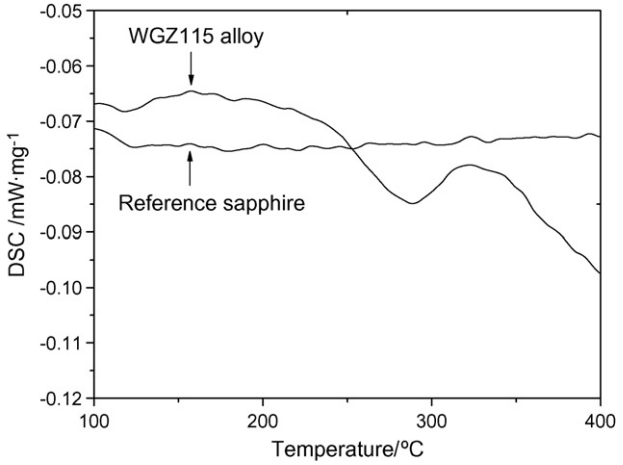

Fig. 2. Curves of DSC of WGZ115 alloy and reference sapphire (100–400 °C).

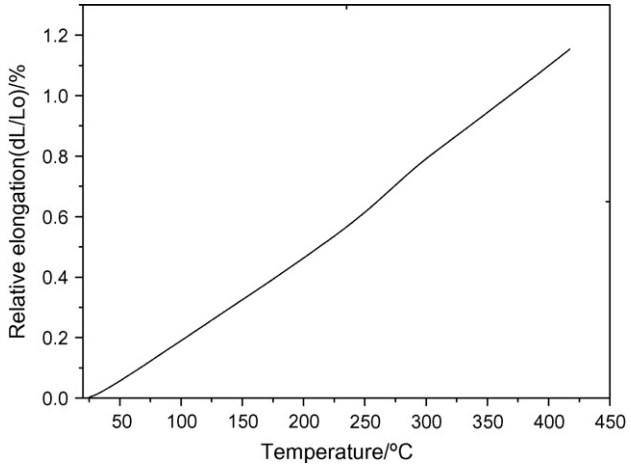

Fig. 4. Relative elongation of WGZ115 alloy (25–400 °C).

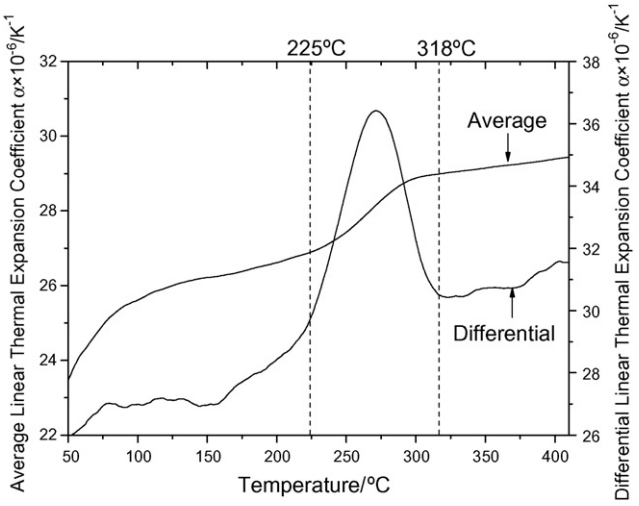

Fig. 5. Linear thermal expansion coefficient of WGZ115 alloy.

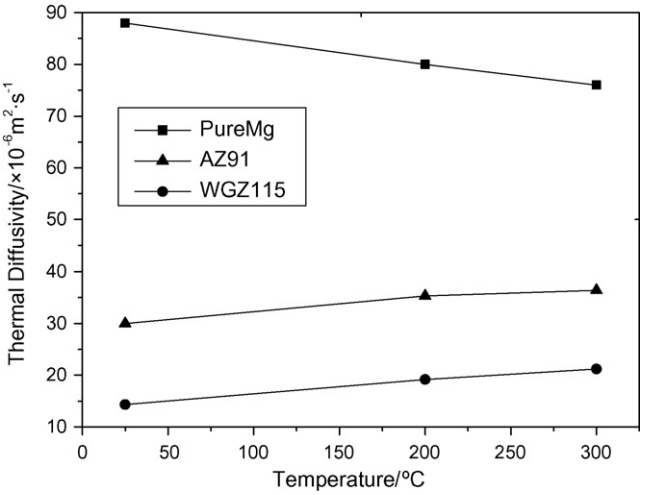

Fig. 6. Thermal diffusivity of WGZ115 alloy, pure Mg and AZ91.

culated as follows [12]:

$$\alpha_a = \frac{L - L_0}{L_0(T - T_0)} = \frac{dL}{L_0 dT} \quad (2)$$

where T_0 is 25 °C, L_0 is the original length of the specimen at T_0, L is the actual length of specimen at T, dL is the elongation at the temperature interval of dT. When dT is infinitely close to 0, it is defined as differential linear thermal expansion coefficient:

$$\alpha_d = \frac{1}{L}\left(\frac{\partial L}{\partial T}\right) \quad (3)$$

The average linear thermal expansion coefficient of WGZ115 alloy in the temperature range of 50–400 °C is represented in Fig. 5. It is indicated that the value of average linear thermal expansion coefficient of WGZ115 alloy increases with increasing temperature. When heating the sample from 50 °C to 75 °C, the rate of thermal expansion increases faster, which could be attributed to the residual stress. Residual stress due to the phases in and around grains is released by increasing temperature. It is evident that the phase transition which occurs between 225 °C and 318 °C has a significant effect on the linear thermal expansion coefficient [13]. The slope of the average linear thermal expansion coefficient curve at the range of 225–318 °C is bigger than that of higher temperatures. The strength of the metallic bond is changed when the temperature is above 318 °C, which makes it easier for the formation of crystal lattice vacancy [14]. So the linear thermal expansion coefficient of WGZ115 alloy is still slowly increasing above 318 °C. At 400 °C the value of average linear thermal expansion coefficient is $29.39 \times 10^{-6}\,K^{-1}$.

The differential linear thermal expansion coefficient curve of WGZ115 alloy is shown in Fig. 5. It has similar trend as that of the specific heat capacity (Fig. 3). There exists a peak between 225 °C and 318 °C. At the same temperature, the value of differential linear thermal expansion coefficient is bigger than that of average linear thermal expansion coefficient.

3.4. Thermal diffusivity and thermal conductivity

Fig. 6 shows the values of the thermal diffusivity of WGZ115 alloy with the literature values of pure Mg and AZ91 alloy for comparison [15,16]. At room temperature the thermal diffusivity is $14.3 \times 10^{-6}\,m^2\,s^{-1}$, while it reaches to $21.2 \times 10^{-6}\,m^2\,s^{-1}$ at 300 °C.

Thermal conductivity values are calculated from the following equation [17]:

$$\lambda = \alpha C_p \rho \quad (4)$$

where λ is the thermal conductivity, α is the thermal diffusivity, C_p is the specific heat capacity, and ρ is the density. The temperature dependence of the density can be estimated as follows:

$$\rho(T) = \frac{\rho_0}{(1 + dL/L_0)^3} \quad (5)$$

where ρ_0 is the density at room temperature and dL/L_0 is the relative elongation (Fig. 4). Fig. 7 shows the values of the thermal conductivity of WGZ115 alloy at three independent different temperatures according to Eq. (4). Literature values of pure Mg and AZ91 alloy are included in the figure for comparison [16,18]. The value increases with increasing temperature from 23.0 W m^{-1} K^{-1} at 25 °C to 40.0 W m^{-1} K^{-1} at 300 °C.

It is well known that magnesium and its alloys have high thermal conductivity and high thermal diffusivity. In general, the more components the alloys contain, the lower the thermal conductivity and thermal diffusivity would be. The reason for that is the solution elements in the alloys act as scattering centers of the phonon and electron contribution to the thermal transfer. Yamasaki et al. [18] discussed that the Mg–RE alloy with Zn additions can form long-

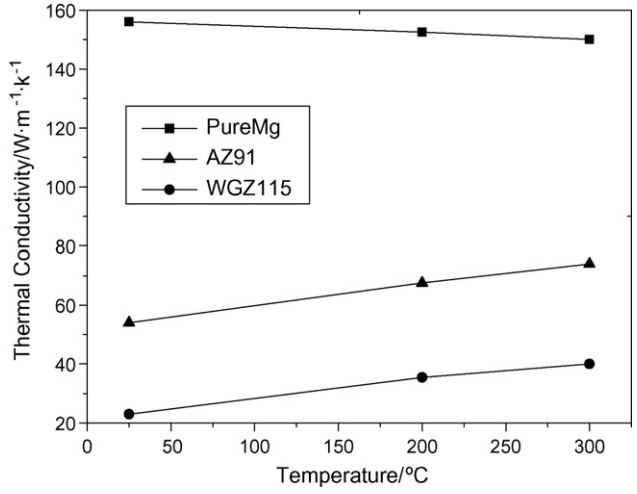

Fig. 7. Thermal conductivity of WGZ115 alloy, pure Mg and AZ91.

Please cite this article in press as: C.J. Chen, et al., J. Alloys Compd. (2009), doi:10.1016/j.jallcom.2009.07.177

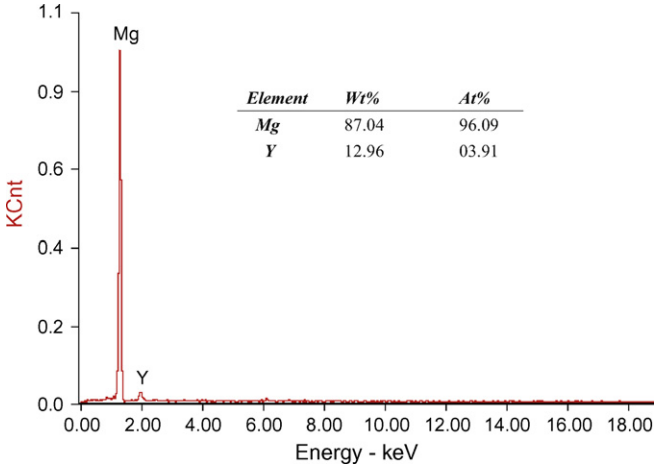

Fig. 8. EDX analysis of the WGZ115 alloy matrix phase.

period stacking ordered structure (LPSO), which consumes the rare earth elements and increase the thermal transfer ability. The element of Zn (0.87 at.%) is also added in the WGZ115 alloy and can only consume Y (0.87at.%) to form the $Mg_{12}Y_1Zn_1$ phase. The matrix still contains a large amount of Y element (3.91 at.%) as is shown in Fig. 8. Rudajevová's [19] research indicates that the transition element Sc can sufficiently reduce and suppress electronic thermal transfer. Y and Sc are in the same column of periodic table of chemical elements. They have similar chemical and physical properties. Y is one of the transition elements which can easily absorb free electrons in the alloy in order to achieve a relatively stable electronic shell. There are less free electrons left for thermal transfer.

4. Conclusions

(1) The specific heat capacity and differential linear thermal expansion coefficient of WGZ115 alloy increase with temperature, except for a peak value in the curve between 225 °C and 318 °C, which is caused by phase transition. Below 225 °C, the deviation is less than 8.5% between calculated and measured values of specific heat capacity.

(2) At room temperature, the value of the thermal conductivity and thermal diffusivity of WGZ115 alloy is 23.0 $W\,m^{-1}\,K^{-1}$ and $14.3 \times 10^{-6}\,m^2\,s^{-1}$, respectively, which is smaller than that of pure Mg and AZ91 alloy. The transition element Y is the main factor to decrease the thermal transformation.

References

[1] Y.C. Guo, J.P. Li, J.S. Li, Z. Yang, J. Zhao, F. Xia, M.X. Liang, J. Alloys Compd. 450 (2008) 446–451.
[2] X.B. Liu, R.S. Chen, E.H. Han, J. Alloys Compd. 465 (2008) 232–238.
[3] K. Liu, J.H. Zhang, D.X. Tang, L.L. Rokhlin, F.M. Elkin, J. Meng, Mater. Chem. Phys. 117 (2009) 107–112.
[4] D.J. Li, X.Q. Zeng, J. Dong, C.Q. Zhai, W.J. Ding, J. Alloys Compd. 468 (2009) 164–169.
[5] Y. Gao, Q.D. Wang, J.H. Gu, Y. Zhao, Y. Tong, D.D. Yin, J. Alloys Compd. 477 (2009) 374–378.
[6] L. Gao, R.S. Chen, E.H. Han, J. Alloys Compd. 481 (2009) 379–384.
[7] S.M. He, X.Q. Zeng, L.M. Peng, X. Gao, J.F. Nie, W.J. Ding, J. Alloys Compd. 427 (2007) 316–323.
[8] N. Žaludavá, Mg–RE alloys and their applications, in: WDS'05 Proceedings of Contributed Papers, Part III, 2005, pp. 643–648.
[9] L.L. Rokhlin, Magnesium Alloys Containing Rare Earth Metals, Taylor and Francis, London, 2003.
[10] A. Rudajevová, M. Staněk, P. Lukáč, Mater. Sci. Eng. A 341 (2003) 152–157.
[11] A. Lindemann, J. Schmidt, M. Todte, T. Zeuner, Thermochim. Acta 382 (2002) 269–275.
[12] C.H. Su, S. Feth, S.L. Lehoczky, Mater. Lett. 63 (2009) 1475–1477.
[13] H.J. Xie, X.C. Wu, Y.A. Min, J. Iron Steel Res. Int. 15 (2008) 56–61.
[14] T.G. Xi, Thermal Properties of Inorganic Materials, Shanghai Scientific and Technical Publishers, Shanghai, 1981.
[15] J.M. Zhou, Y. Yang, M. Lamvik, G. Wang, J. Cent. South Univ. Technol. 8 (2001) 60–63.
[16] A. Rudajevová, J. Kiehn, K.U. Kainer, B.L. Mordike, P. Lukác, Scr. Mater. 40 (1999) 57–62.
[17] A. Rudajevová, P. Lukáč, Phys. Stat. Sol. A 175 (1999) 457–466.
[18] M. Yamasaki, Y. Kawamura, Scr. Mater. 60 (2009) 264–267.
[19] A. Rudajevová, F.V. Buch, B.L. Mordike, J. Alloys Compd. 292 (1999) 27–30.